

# OFDMA UPLINK CHANNEL PREDICTION TO ENABLE FREQUENCY-ADAPTIVE MULTIUSER SCHEDULING

Daniel Aronsson and Mikael Sternad

Signals and Systems, Uppsala University  
Box 534. 751 21 Uppsala, Sweden, {dar, ms}@signal.uu.se

## ABSTRACT

Frequency-adaptive multiuser scheduling utilizes the frequency-selective small-scale fading to allocate sub-carriers with advantageous signal-to-noise ratio to each user. Due to channel time-variability and delays of the transmission control loop, this will in general require channel prediction. FDD (Frequency Division Duplex) uplinks pose the most challenging prediction problem: All sub-bands that may potentially be allocated must here be predicted for all involved user terminals, based on pilots transmitted from all terminals. This poses challenges with respect to prediction accuracy, estimator complexity and pilot overhead. This paper explores the design of Kalman predictors used for uplink prediction, in the context of the EU WINNER project baseline design system. The paper investigates how the performance depends on the type of pilots that are transmitted from each terminal. The conclusion is that for frequency-selective channels, the use of overlapping pilots outperforms schemes where each user places pilots on exclusive time-frequency symbols. Another conclusion is that cycling the pilot patterns in time improves the performance. Channel prediction in an environment with flat Doppler spectrum is also evaluated. The resulting performance is adequate for use at vehicular velocities at 3-5 GHz carriers.

## 1. INTRODUCTION

The use of OFDMA (Orthogonal Frequency Division Multiple Access) on wide-band channels enables the allocation of users to the frequency regions that are most advantageous for them. A multiuser scheduler could allocate the transmission to/from each users to appropriate frequency bands, by utilizing the channel variations due to the small-scale frequency selective fading. Channels to/from each user will in general vary independently. Substantial multiuser scheduling gains can be attained if each of  $k$  users on average is allocated to the fraction  $1/k$  of the subcarriers that will have highest SINR (signal to interference and noise ratio) for that particular user. Additional (but smaller) gains are obtained by using link adaptation that is adjusted to each allocated subcarrier.

Due to these potential gains, frequency-adaptive transmission in OFDMA downlinks is of interest in the research community, in the ongoing 3GPP long-term evolution (LTE) standardization effort, for WiMAX and in the European beyond-3G WINNER project [1]. One complication in such systems is that for moving terminals, measurements of the channel gain for a subcarrier will become quickly outdated. Fig. 1 illustrates the variation of received power with time and frequency for one particular user and fading pattern.

Frequency-adaptive transmission for vehicular users would therefore require low latency control loops for the

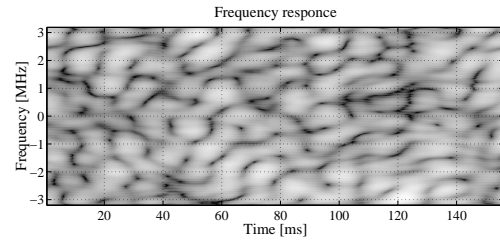


Figure 1: Time-frequency representation of an estimated channel obtained from measurement data on a 6.4 MHz channel at a 1880 MHz carrier. White color denotes high power whereas dark color denotes low power. The dynamic range and the speed of the mobile is approximately 40 dB and 50 km/h, respectively. The coherence bandwidth is 0.6 MHz in this example.

transmission and also efficient channel prediction of the SINR at the instant of transmission. Designs for downlinks up to 100 km/h at 2 GHz carrier have been investigated within the Swedish Wireless IP project [2] and downlink designs targeted at up to 70 km/h at 5 GHz have been proposed and evaluated within the WINNER project [3, 4].

For FDD downlinks and TDD (time division duplex) uplinks and downlinks, channel prediction can be based on downlink pilots that are transmitted by the base station to all terminals within a sector or beam.<sup>1</sup> Channel predictors at each terminal may then predict the frequency selective channel over a band of interest [5, 6]. Suitably compressed messages are reported to the scheduler at the base station. The scheduler then allocates the use of each sub-band of the downlink transmission.

The potential multiuser scheduling gain is as large in FDD uplinks as in the cases outlined above, but the channel prediction problem becomes much harder: FDD uplinks cannot be predicted based on downlink pilots, because uplinks and downlinks work at significantly different carrier frequencies. Predictors at the base station would have to estimate the channels from all terminals who compete for a set of transmission resources. To support this prediction, *all* of these terminals would have to send special-purpose pilots within *all* resources of interest, at an appropriate channel sampling rate.<sup>2</sup> The need for such special uplink pilots leads to two

<sup>1</sup>In TDD, prediction of the downlink channel gains can be used also for the uplink gains, due to the channel reciprocity.

<sup>2</sup>If only the pilots that are embedded in uplink payload transmissions are used, then the channel sampling would depend on the availability and scheduling of the uplink transmissions. Extrapolation to other frequency bands beyond the correlation bandwidth could not be performed. Also, the sampling in any given band could not be relied on to have sufficient rate to support a reliable prediction of the channel in that band.

problems that become severe when the number of competing users is large:

1. If uplink pilots are transmitted in orthogonal positions, then the overhead of earmarked pilot positions relative to payload could become unacceptably large.
2. If  $k$  users compete for a set of resources, each of them will on average obtain only  $1/k$  of the resources but will still have to transmit pilots in all of them. For large  $k$ , this pilot power overhead will negate the multiuser scheduling throughput gains.

The multiuser scheduling gains increase significantly with  $k$  for small  $k$  but slower for large  $k$ . This makes it possible to handle both of the problems outlined above by partitioning the total bandwidth into a number of *competition bands*, each with a limited number, typically  $k = 8$  or less, users. The competition bands should be composed of frequency resources that are well spread out over the uplink bandwidth, to sample the available frequency selectivity.

Our problem here will therefore be to design and assess channel predictors that work on uplink pilots that are transmitted from  $k$  users, within a subset of OFDM subcarriers that constitute a competition band.

We will discuss design aspects for Kalman-based schemes that produce MMSE estimates of the complex frequency-domain channel gains. Compared to Wiener filtering [7, 8], Kalman estimators provide better initial transient accuracy and are the optimal estimators for linear signal models and Gaussian noise. Kalman predictors also provide the prediction covariances. The quantified uncertainty can be used by the scheduler and by the link adaptation, to e.g. attain a target bit error rate at a given prediction variance [9].

The Kalman predictors can be implemented in the time domain, by tracking impulse response coefficients and then transforming them to predicted frequency domain channels. Alternatively, they can be implemented in the frequency domain. The performance of both these schemes has been evaluated, and is identical. We here show the results from the frequency domain implementation.

Initial results on Kalman-based predictors for FDD uplinks were reported in [10] and [3]. We will here discuss the effects of different pilot patterns on the performance. Channel prediction in an environment with flat Doppler spectrum is also evaluated.

## 2. SYSTEM MODEL

The performance will be evaluated with respect to the baseline system design of the WINNER FDD mode [11]. This design has a system sampling period of 12.5 ns, giving a FFT bandwidth of 80 MHz. The signal bands are 45 MHz in both uplinks and downlinks. Each OFDM symbol is 2048 samples plus an additional 256 samples for the cyclic prefix. The subcarrier width is 39.06 kHz and the OFDM symbol + guard duration is 28.8  $\mu$ s.

The time-frequency radio resource is divided into blocks (chunks) of 8 subcarriers (312.5 kHz) by 12 OFDM symbols (345.6  $\mu$ s). A chunk duration is denoted a *slot*. These chunks constitute the unit for frequency-adaptive resource allocation. The chunk size is selected to make the channel moderately flat within chunks. Uplink pilot symbols known to the receiver facilitate the prediction. They are here assumed to be located on one of the 12 OFDM symbols. We

here also assume a full-duplex FDD uplink, so uplink pilots will be transmitted within each slot.

To prepare for frequency adaptive uplink transmission, the terminal is allocated a competition band and begins to send pilots in that band. Based on these pilots, an autoregressive model is adjusted to the temporal correlation (Doppler spectrum) and the frequency correlation of the fading is also estimated. These models are input data to the predictors and are used for assessing the attainable prediction accuracy.

Channel predictions are then produced for this users channel (see Section 3 below). When a packet for uplink transmission arrives, the terminal sends a transmission request during slot  $j$ . The scheduler may grant the request and sends the allocation information over a downlink control channel during slot  $j + 1$ . The transmission then commences over the uplink in slot  $j + 2$ . The required prediction horizon is two slots, or 0.7 ms, or  $L = 2$  channel samples. This tight control loop requires the update of the channel prediction from the last measurement in slot  $j$ , the scheduling and the downlink control transmission to be executed within less than 1.5 slot durations (0.5 ms).

## 3. STATE SPACE MODELLING

We construct a linear filter that uses measurements of  $W$  parallel pilot-bearing subcarriers. The fading taps of  $U$  simultaneous users<sup>3</sup> are modeled by

$$\begin{aligned} x_{t+1} &= Fx_t + Gu_t, \\ h_t &= Hx_t \end{aligned} \quad (1)$$

$$\{F, G, H\} = \text{diag}_{\#users}(\text{diag}_{\#subc.}(\{F_s, G_s, H_s\})).$$

Here,  $\text{diag}_a$  is a block diagonal matrix holding  $a$  blocks, and  $h_t$  is a vector holding the  $W \times U$  fading taps. Each triplet  $\{F_s, G_s, H_s\}$  models the fading statistics of one tap with an autoregressive model of order 4. The four poles of this model are so chosen as to represent a Doppler spectrum, in general different for different terminals. The shape of the Doppler spectrum depends on the fading environment. When not explicitly stated otherwise, a flat Doppler spectrum in  $[-f_D, f_D]$ , where  $f_D$  is the maximal Doppler frequency is used in this paper.

The vector  $y_t$  of the  $W$  received signals at the time-frequency pilot positions is modeled by placing the pilots of each user  $j$  at time  $t$  in diagonal  $W \times W$  matrices  $\{\psi_{j,t}\}$  and writing

$$y_t = \text{stack}_{\#users}(\psi_{j,t})h_t + v_t. \quad (2)$$

Here,  $\text{stack}_a$  is a matrix of  $a$  blocks stacked horizontally, and  $v_t$  represents noise and interference. Note that, unless we set most pilot symbols to zero, the received signal at a subcarrier will be affected by the channels from multiple users.

The correlation between the taps is expressed by the process noise covariance matrix  $Q = Eu_t u_t^*$ , while  $R = Ev_t v_t^*$  is the noise covariance matrix. Here, we will assume  $R = \sigma_n^2 I$ .

With the state and measurement equations (1) and (2), optimal inferences about the taps  $h$  are obtained by the Kalman equations. See e.g. [12]. The  $L$ -step prediction estimate of  $h$  is obtained from the state estimate  $\hat{x}_{t|t}$  by

$$\hat{h}_{t+L|t} = HF^L \hat{x}_{t|t}.$$

<sup>3</sup>Channels for multiple transmit antennas/spatial streams from one terminal are here modelled as channels from different users.

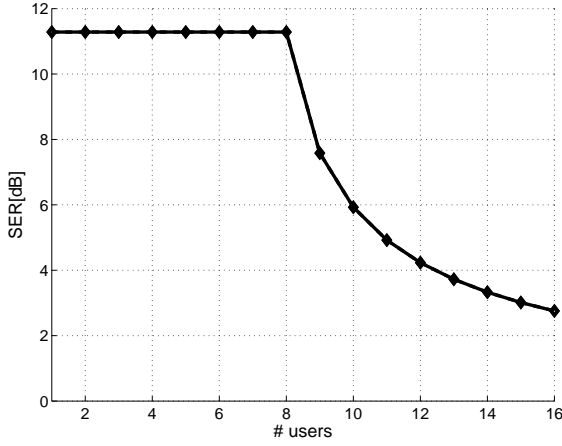


Figure 2: Two-step ( $L=2$ ) prediction performance versus number of users for dedicated (dashed line) and overlapped (solid line) pilots on flat fading channels. The lines overlap. Average  $E_s/N_0 = 12$  dB.

The attainable prediction accuracy will depend on the prediction horizon  $\ell$  scaled in carrier wavelengths, which in turn depends on the terminal velocity  $v$ , the prediction horizon in time  $Lt_p$  [s] and the carrier wavelength  $\lambda_c$  via the relation  $\ell = vLt_p/\lambda_c$ . In the assumed WINNER baseline design, the horizon is  $L = 2$ , the sampling time  $t_p$  equals the slot duration ( $345.6 \mu\text{s}$ ) and  $\lambda_c = 8.1$  cm (3.7 GHz uplink carrier).

#### 4. PILOTS

One may adjust the dimensionality of  $y$  or the filter width (here denoted  $W$ ), i.e. the number of simultaneous subcarriers to be tracked, depending on the performance/complexity tradeoff. A competition band that comprises  $C$  predicted subcarriers will then require the use of  $\text{int}[C/W]$  Kalman predictors run in parallel.

The pilots  $\{\psi_i\}$  are also design parameters. Should the pilot symbols transmitted by each user be placed on all  $W$  subcarriers that are tracked, hence making the pilots from the different users overlap? Or should we instead use dedicated pilots, so that each user concentrates its pilot energy to one single subcarrier, not transmitting anything on the remaining  $W - 1$  subcarriers?

Assuming that the number of users  $U$  in the competition band is less or equal to the number of subcarriers  $W$ , we may represent the the pilots used by up to  $W$  users by a  $W \times W$ -matrix  $\Psi$ , where each column contains the complex-valued time-frequency pilots for one user. The diagonal of the diagonal matrices  $\{\psi\}$  in (2) are then constructed from the columns of  $\Psi$ . *Dedicated* pilots are simply obtained through  $\Psi = \sqrt{W}\mathbf{I}_W$ , where  $\mathbf{I}$  denotes the identity matrix. *Overlapping* pilots are constructed through  $\Psi = \text{hadamard}(W)$ .

Although complex hadamard matrices are possible to find, they have no advantage over real matrices. We will here use Sylvester's construction which yields pilot symbols of either  $-1$  or  $1$ , i.e. BPSK symbols. Hence we construct a  $2^n \times 2^n$  Hadamard matrix by setting  $H_0 = 1$  and iterating

$$H_{n+1} = \begin{pmatrix} H_n & H_n \\ H_n & -H_n \end{pmatrix} \quad (3)$$

It is not possible to construct more than  $W$  real or complex-

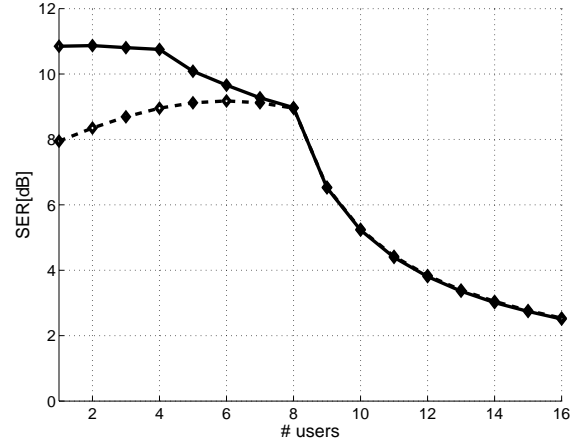


Figure 3: Two-step ( $L=2$ ) prediction performance versus number of users for dedicated (dashed line) and overlapped (solid line) pilots on frequency selective channels. WINNER C2 channel model and time-invariant pilot patterns. Kalman estimators track  $W = 8$  adjacent subcarriers. Average  $E_s/N_0 = 12$  dB, velocity 50 km/h, 3.7 GHz carrier.

valued orthogonal pilot sequences. If the number of users is greater than the filter width  $W$ , we therefore need to construct additional non-orthogonal pilot sequences from the orthogonal set  $\Psi$ . There is no general scheme for how to do this optimally. In this paper we construct new pilots by pairwise combining pilots from the original set and multiplying the sum with  $1/\sqrt{2}$  to normalize the pilot symbols to preserve energy. The matrix used here that maps 8 orthogonal pilots onto 16 non-orthogonal pilots is

$$\mathbf{I}_8 \begin{bmatrix} \alpha & \alpha & \cdot & \alpha & \cdot & \cdot & \alpha & \cdot \\ \alpha & \cdot & \alpha & \cdot & \alpha & \cdot & \cdot & \alpha \\ \cdot & \alpha & \alpha & \cdot & \cdot & \alpha & \cdot & \cdot \\ \cdot & \cdot & \cdot & \alpha & \alpha & \alpha & \cdot & \cdot \\ \cdot & \cdot & \cdot & \cdot & \cdot & \cdot & \alpha & \alpha \\ & & & & & & & 3 \times 8 \text{ zeros} \end{bmatrix} \quad (4)$$

where  $\mathbf{I}_8$  is the  $8 \times 8$  identity matrix, and  $\alpha = 1/\sqrt{2}$ .

## 5. RESULTS

### 5.1 Channel model

The results in this section are evaluated on two channel models: A flat (frequency non-selective) channel, and a frequency selective non-line-of sight channel for urban environments (WINNER C2 channel) with power delay profile

Delay[ns]	Power[dB]
0, 5, 135, 160, 215, 260,	-0.5, 0.0, -3.4, -2.8, -4.6, -0.9,
385, 400, 530, 540, 650,	-6.7, -4.5, -9.0, -7.8, -7.4,
670, 720, 750, 800, 945,	-8.4, -11.0, -9.0, -5.1, -6.7,
1035, 1185, 1390, 1470	-12.1, -13.2, -13.7, -19.8

When not explicitly stated otherwise, we set the velocity of the terminals to 50 km/h, the average signal-to-noise ratio  $E_s/N_0$  to 12 dB, and the filter width  $W$  to 8 subcarriers (one chunk width). The estimation horizon is set to two steps (slots). Performance is expressed either in terms of the mean value over all  $W \times U$  channel taps of the signal-to-estimation error power ratio (SER), or by the normalized mean square error  $\text{NMSE} = (\text{SER})^{-1}$ .

## 5.2 Overlapping pilots

In a general FDD uplink wireless scenario, the channels between terminals and base station will be frequency selective. As previously noted, the base station has to estimate these channels to a certain precision in order to be able to schedule resources efficiently. On one hand, the use of overlapping pilots will provide the base station with information of the entire filter bandwidth for all users simultaneously. The fact that users send pilots at the same time-frequency slots will however degrade performance as compared to the scenario where each user has dedicated slots for its pilots. The use of dedicated pilots will on the other hand give poor information about how the channel varies over different frequencies.

We compare the performance of overlapped pilots against the performance of dedicated pilots. Figure 2 shows SER versus number of users  $U$  when the channels experienced by the users are flat and the filter width is set to  $W = 8$ . Here we turn our attention only to the case  $U \leq W$ . All subcarriers fade in unison and the pilots for users 1 through 8 are completely orthogonal. In the noise-free case, the  $W$  measurements provided at time  $t$  by eq. (2) would then provide a solvable linear system of equations with respect to the  $U \leq W$  different channel coefficients. This holds regardless of whether we use overlapped or dedicated pilots.<sup>4</sup> When the channels are flat fading we therefore have the result that

- the choice of pilots is irrelevant as long as the pilots are orthogonal, and
- the performance does not degrade with an increasing number of users  $U$  as long as  $U \leq W$ .

The situation is vastly different when the channels are frequency selective. The importance of measuring over the entire filter bandwidth is evident when we study Figure 3 for users 1–8. For the particular working point  $E_s/N_0 = 12$  dB studied here, the gain is about 3 dB for one user, and decreases when the number of simultaneous users increases.

The curves merge at the point  $U = 8$ , indicating that the choice of pilots is unimportant when the orthogonal set has been filled. This conclusion should however be drawn with care, because in the dedicated case, the SER will vary considerably, from high (on the carrier over which pilots are transmitted), to low (on carriers far from the pilot carrier). Since modulation format is selected per chunk, one would prefer a more even distribution of the SER, such as is produced by the overlapping pilots.

The reason for the performances for dedicated pilots (dashed) actually *increasing* with  $U$  is due to the way the pilot subcarriers have been allocated to users in this experiment. The first user here puts pilot energy on the first subcarrier, which is on the border of the filter bandwidth, while users 4 and 5 invest their pilots in the middle of the bandwidth. The latter is the better tactic when we rate performance based on the mean value of the SER over all subcarriers. This is the reason for the performance increase when users 2, 3 and so on are added to the system.

<sup>4</sup>In that case,  $h_t = \text{diag}_U(\mathbf{1}_W)\bar{h}_t$ , where  $\bar{h}_t = (\bar{h}_t^{(1)}, \dots, \bar{h}_t^{(U)})^T$ , where  $\bar{h}_t^{(j)}$  is the flat-fading scalar channel coefficient for user  $j$  and  $\mathbf{1}_W$  is a column vector of  $W$  ones. In the noise-free case, (2) then gives

$$y_t = \text{stack}_U(\psi_{j,t})h_t = \text{stack}_U(\psi_{j,t})\text{diag}_U(\mathbf{1}_W)\bar{h}_t = \Psi_{W \times U}\bar{h}_t,$$

where  $\Psi_{W \times U}$  equals the first  $U$  columns of the matrix  $\Psi$  introduced in Section 4, which, by construction, will have full rank  $U$ .

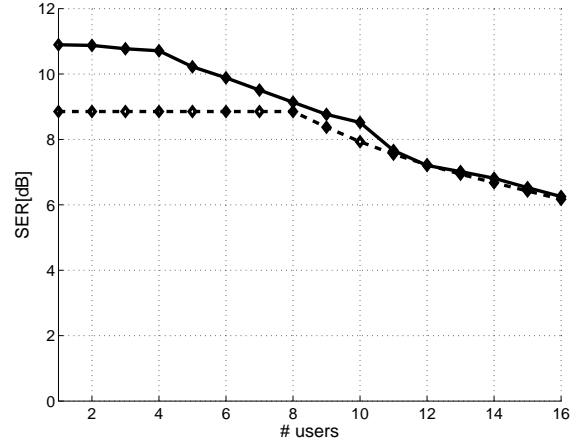


Figure 4: Two-step ( $L=2$ ) prediction performance versus number of users for dedicated (dashed line) and overlapped (solid line) pilots on frequency selective channels. Conditions as in Figure 3, but here the pilot patterns of each user cycle over time with period 8.

This illustrates that if dedicated (and time static) pilots are to be used, then one should assign one of the middle subcarriers to the first user to enter the system, and only assign border subcarriers when necessary.

## 5.3 Cyclic pilots

When the number of users  $U$  to share a certain bandwidth is larger than the corresponding filter width  $W$ , it is not possible to find a set of  $U$  orthogonal pilots. As presented in Section 4, we then construct new pilots from the original set of  $W$  orthogonal pilots by weighing together them two by two. Restudying Figures 2 and 3, we note two facts. One is that the performance drop when we go from orthogonal to non-orthogonal pilots ( $U = 8$  to  $U = 9$ ) is considerable. The other fact is that the performance is unaffected by the choice of dedicated versus overlapping pilots.

The performance can be improved by providing the filter with more information about the time variability of the channels. We have seen that the filtering performance increases if we spread out the pilot energy and let the pilots vary over the different frequencies in the frequency band. In the same manner we may design the pilots to make optimal use of previous channel samples. In the case of noiseless, *frequency-selective but time-invariant* channels (i.e. immobile terminals), we would obtain a linear system of equations

$$Y = Ah \quad (5)$$

where  $A = [\text{stack}_U(\psi_{j,t})^T \dots \text{stack}_U(\psi_{j,t+W-1})^T]^T$ ,  $Y = (y_t^T, \dots, y_{t+M-1}^T)^T$  and  $h_t = h$ . If a set of orthogonal pilots is cycled over time so that  $A$  obtains full rank  $WU$ , the system (5) becomes solvable. That should improve the estimation also for time-varying channels and noisy measurements.

For *dedicated* pilots, this property is obtained for  $M = 8$  by simply rotating the original  $\Psi_{t=0} = \sqrt{8}\mathbf{I}_8$  one step left every time step, hence producing all eight time steps.

Time varying *overlapping* pilots are constructed as follows. We here study the specific case  $U \leq 8$ . For the first time step we use the same Hadamard matrix as used for the

static pilots:

$$\Psi_{t=0} = \begin{bmatrix} 1 & 1 & 1 & 1 & 1 & 1 & 1 & 1 \\ 1 & -1 & 1 & -1 & 1 & -1 & 1 & -1 \\ 1 & 1 & -1 & -1 & 1 & 1 & -1 & -1 \\ 1 & -1 & -1 & 1 & 1 & -1 & -1 & 1 \\ 1 & 1 & 1 & 1 & -1 & -1 & -1 & -1 \\ 1 & -1 & 1 & -1 & -1 & 1 & -1 & 1 \\ 1 & 1 & -1 & -1 & -1 & -1 & 1 & 1 \\ 1 & -1 & -1 & 1 & -1 & 1 & 1 & -1 \end{bmatrix} \quad (6)$$

$$= [\Psi_1 \ \Psi_2 \ \Psi_3 \ \Psi_4 \ \Psi_5 \ \Psi_6 \ \Psi_7 \ \Psi_8],$$

where  $\Psi_i$  is the pilot pattern used by user  $i$  at time  $t = 0$ . This Hadamard matrix is then used a second time to construct all time steps. In the resulting matrix below, each row correspond to one time step  $t = 0, 1, \dots, 7$ .

$$\begin{bmatrix} \Psi_1 & \Psi_2 & \Psi_3 & \Psi_4 & \Psi_5 & \Psi_6 & \Psi_7 & \Psi_8 \\ \Psi_1 & -\Psi_2 & \Psi_3 & -\Psi_4 & \Psi_5 & -\Psi_6 & \Psi_7 & -\Psi_8 \\ \Psi_1 & \Psi_2 & -\Psi_3 & -\Psi_4 & \Psi_5 & \Psi_6 & -\Psi_7 & -\Psi_8 \\ \Psi_1 & -\Psi_2 & -\Psi_3 & \Psi_4 & \Psi_5 & -\Psi_6 & -\Psi_7 & \Psi_8 \\ \Psi_1 & \Psi_2 & \Psi_3 & \Psi_4 & -\Psi_5 & -\Psi_6 & -\Psi_7 & -\Psi_8 \\ \Psi_1 & -\Psi_2 & \Psi_3 & -\Psi_4 & -\Psi_5 & \Psi_6 & -\Psi_7 & \Psi_8 \\ \Psi_1 & \Psi_2 & -\Psi_3 & -\Psi_4 & -\Psi_5 & -\Psi_6 & \Psi_7 & \Psi_8 \\ \Psi_1 & -\Psi_2 & -\Psi_3 & \Psi_4 & -\Psi_5 & \Psi_6 & \Psi_7 & -\Psi_8 \end{bmatrix} \quad (7)$$

The impact of using cyclic pilots is studied in Figure 4. When the number of simultaneous users  $U$  is less or equal to eight, the only improvement is an averaging of the performance for the dedicated pilots as compared to the case when static pilot positions were used (Figure 3).

When  $U \geq 9$  the improvement is more dramatic. The steep performance drop at  $U = 9$  is now gone. We conclude that the use of cyclic pilots is highly important to maintain a high estimation performance when the number of users competing for a frequency band is larger than the bandwidth  $W$ .

#### 5.4 Prediction over Scheduling Time-Horizons

To allow for efficient scheduling of resources, the channels need to be predicted. We evaluate the prediction performance for different signal-to-noise ratios ( $E_s/N_0$ ). Results for flat Doppler spectra are presented in Figure 5. Acceptable predictability for frequency adaptive transmission is obtained when the NMSE is below 0.15 [3, 4]. From the expression for calculating the prediction horizon in Section 3,  $\ell = \nu L t_p / \lambda_c$ , the required prediction horizon is, for example,  $\ell = 0.12$  when  $\nu=50$  km/h and  $L = 2$ . Hence, the minimal acceptable prediction performance is obtained when  $E_s/N_0 > 10$  dB.

The channel predictability depends largely on the Doppler spectrum. Flat Doppler spectra give channels with the worst predictability. Channels with Doppler spectra with pronounced peaks are easier to predict.<sup>5</sup> Use of the Jakes model, which corresponds to isotropically placed scatterers in two dimensions, was evaluated in Figure 3.5 of [3], for  $U = 8$  uplink users. It results in lower prediction NMSEs relative to Figure 5, e.g. NMSE 0.15 for  $\ell = 0.12$  at 3 dB.

The obtained levels of predictability are adequate for link adaptation and multiuser scheduling, with the assumed tight feedback control loop, at carrier frequencies of 3-5 GHz.

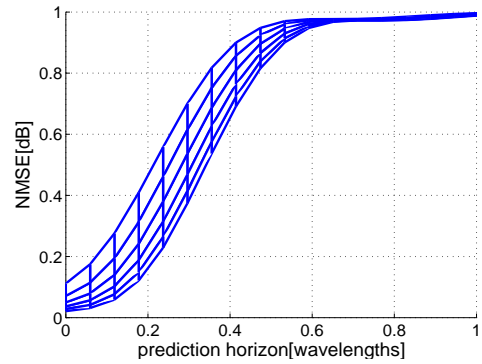


Figure 5: The predictor performance for flat Doppler spectrum measured by the NMSE versus prediction horizon measured in wavelengths. The signal-to-noise ratio  $E_s/N_0$  goes from 0 dB (upper curve) to 25 dB (lower curve) in steps of 5 dB.  $U = 8$  users with overlapping pilots,  $W = 8$ , WINNER C2 channel model.

#### REFERENCES

- [1] IST WINNER and WINNER II projects, partly funded by the European Commission. Online: <https://ist-winner.org><sup>6</sup>
- [2] M. Sternad, T. Ottosson, A. Ahlén and A. Svensson, "Attaining both coverage and high spectral efficiency with adaptive OFDM downlinks," *VTC 2003-Fall*, Orlando, Fla, Oct. 2003.
- [3] IST-2003-507581 WINNER, "D2.4: Assessment of Adaptive Transmission Technologies," Feb. 2005. Available on <https://ist-winner.org>.
- [4] M. Sternad, S. Falahati, T. Svensson and D. Aronsson, "Adaptive TDMA/OFDMA for wide-area coverage and vehicular velocities," *IST Mobile and Vehicular Summit*, Dresden, June 19-23 2005.
- [5] T. Ekman *Prediction of Mobile Radio Channels. Modeling and Design* PhD Thesis, Signals and Systems, Uppsala University, Sweden, 2002. Online: [www.signal.uu.se/Publications/abstracts/a023.html](http://www.signal.uu.se/Publications/abstracts/a023.html)
- [6] M. Sternad and D. Aronsson, "Channel estimation and prediction for adaptive OFDM downlinks," *IEEE VTC 2003-Fall*, Orlando, Fla, Oct. 2003.
- [7] P. Hoeher, S. Kaiser and P. Robertson, "Two-dimensional pilot-symbol-aided channel estimation by Wiener filtering," *IEEE ICASSP*, 1997, pp. 1845-1848.
- [8] G. Auer, "Analysis of pilot-symbol aided channel estimation for OFDM systems with multiple transmit antennas," *IEEE Intern. Conf. on Commun. ICC 04*, Paris, June 2004.
- [9] S. Falahati, A. Svensson, M. Sternad and T. Ekman, "Adaptive modulation systems for predicted wireless channels," *IEEE Trans on Commun.*, vol. 52, pp. 307-315, Feb. 2004.
- [10] M. Sternad and D. Aronsson, "Channel estimation and prediction for adaptive OFDMA/TDMA uplinks based on overlapping pilots," *IEEE ICASSP*, Philadelphia, March 19-23 2005.
- [11] IST-4-027756 WINNER II, "D6.13.7: Test Scenarios and Calibration Cases; Issue 2," Dec. 2006. Available on <https://ist-winner.org>.
- [12] T. Kailath, A.H. Sayed and B. Hassibi, *Linear Estimation* Prentice-Hall, Upper Saddle River, NJ, 2000.

<sup>5</sup>An illustration of the wide range of predictabilities obtained for measured channels can be found in Fig 6.15 of [5].

<sup>6</sup>This work has been partially performed within the project IST-3-027756 WINNER II, which is partially funded by the European Union. The authors wish to acknowledge the contributions of their colleagues. It was also partially funded by the Swedish Foundation of Strategic Research.